Synthesis and Structural Analysis of Iron Doped Zinc Oxide Nanoparticles

RUBY CHAUHAN[1], ASHAVANI KUMAR[2,*] and RAM PAL CHAUDHARY[1]

[1]Department of Chemistry, Sant Longowal Institute of Engineering and Technology, Longowal-148 106, India
[2]Department of Physics, National Institute of Technology, Kurukshetra-136 119, India

*Corresponding author: Fax: +91 1744 233495; Tel: +91 1744 233495; E-mail: ashavani@yahoo.com

Nanocrystals of undoped and iron doped zinc oxide ($Zn_{1-x}Fe_xO$, where x = 0.00 to 0.05) were synthesized by coprecipitation method. Crystalline phases and optical absorption of prepared samples were determined by X-ray diffraction and UV-visible spectrophotometer. The average particles size was determined from X-ray line broadening. X-ray analyses revealed the formation of the hexagonal wurtzite ZnO with secondary phase in the Fe-doped sample. The incorporation of iron in place of zinc provoked an increase in the size of nanocrystals as compared to undoped ZnO. Crystalline size of nanocrystals varied from 27 to 41 nm as the calcinations temperature increased. Optical absorption measurement indicated red shift in the absorption band edge upon Fe doping. The band gap value was found to decrease from 2.90 to 2.85 eV with iron (5 %) doping at 800 ℃.

Key Words: Nanoparticles, Coprecipitation, XRD, UV-VIS spectrophotometer.

INTRODUCTION

Nanocrystalline materials have attracted a wide attention due to their unique properties and immense potential application in nano device fabrication[1-4]. Zinc oxide (ZnO), a direct wide bandgap (3.4 eV at room temperature) II-VI compound n-type semiconductor, has a stable wurtzite structure with lattice spacing a = 0.325 nm and c = 0.521 nm and composed of a number of alternating planes with tetrahedrally-coordinated O^{2-} and Zn^{2+} ions, stacked alternately along the c-axis. It has attracted intensive research effort for its unique properties and versatile applications in transparent electronics, ultraviolet (UV) light emitters, piezoelectric devices, chemical sensors and heterogeneous photocatalysts[5-15]. It has been proposed to be a more promising UV emitting phosphor than GaN because of its larger exciton binding energy (60 meV). All these predominant properties make ZnO a great potential in the field of nanotechnology.

Various chemical methods have been developed to prepare nanoparticles of different materials of interest. Most of the ZnO crystals have been synthesized by traditional high temperature solid state method; in which, it is difficult to control the particle properties and also energy consumption. ZnO nanoparticles can be prepared on a large scale at low cost by simple solution based method, such as chemical precipitation, sol-gel synthesis and hydrothermal reaction[16-21]. Many of the earliest synthesis of nanoparticles were achieved by coprecipitation of sparingly soluble products from aqueous solution followed by thermal decomposition of those products to oxides. Coprecipitation method is a promising alternative synthetic method because of the low process temperature and easy to control the particle size. Some of the most commonly substances used in coprecipitation operations are hydroxides, carbonates, sulphates and oxalates. Mandal found that the formation of a secondary phase in transition metal ion doped ZnO powders was dependent on the level of doping and preparation temperature[22].

In the present work undoped and Fe doped ZnO nanoparticles ($Zn_{1-x}Fe_xO$, where x = 0.00 to 0.05) were synthesized by chemical coprecipitation method, which is robust and reliable to control the shape and size of particles without requiring the expensive and complex equipments[23].

EXPERIMENTAL

All chemicals were of analytical grade from Fisher Scientific and used without further purification. X-Ray Diffraction (XRD) patterns were recorded on a Rigaku mini desktop diffractometer using graphite filtered CuK$_\alpha$ radiation ($\lambda = 1.54$ Å) at 40 KV and 100 mA with scanning rate of 3 degree per minute (from $2\theta = 20$ to $80°$). Optical absorption spectra were recorded on Shimadzu double beam double monochromator spectrophotometer (UV-2550), equipped with integrated sphere assembly ISR-24 Å in the range of 190 to 900 nm.

Coprecipitation method (preparation of undoped and iron doped zinc oxide nanoparticles): The starting materials,

$ZnSO_4 \cdot 7H_2O$ and $FeSO_4 \cdot 7H_2O$ solution were prepared as follows: Solution-A: 0.1M $ZnSO_4 \cdot 7H_2O$ dissolved in distilled water and solution-B: 0.1M $FeSO_4 \cdot 7H_2O$ in distilled water. Mixing these solutions has resulted solution-C. The experiment was performed at room temperature. Separately, a buffer solution (pH = 4.6) was prepared by dissolving appropriate amounts of sodium hydroxide and sodium carbonate in distilled water. The pH of buffer solution was selected so as to cause precipitation of the iron carbonate/ basic zinc carbonate from the solution-C. Buffer solution was then added drop wise to the vigorously stirred solution-C to produce a brown/white, gelatinous iron carbonate/basic zinc carbonate precipitate. After addition of the reagents, the mixture was stirred for 2 h at room temperature. The precipitate was filtered and washed with distilled water. The precipitate was dry at 110 ºC for 2 h and calcinations were performed at 800 ºC and 1000 ºC in muffle furnace. The iron carbonate/ basic zinc carbonate precipitate was decomposed in iron doped zinc oxide.

RESULTS AND DISCUSSION

X-ray diffraction studies: Fig. 1(a) and (b) show the XRD diffraction patterns of undoped and iron doped zinc oxide ($Zn_{1-x}Fe_xO$, where x = 0.00 to 0.05) powder samples at 800 and 1000 ºC temperatures indicated coexistence of wurtzite Zn(Fe)O and spinel $ZnFe_2O_4$ phase. In present case, all the diffraction peaks at angles (2θ) of 31.36, 34.03, 35.86, 47.16, 56.26, 62.54, 67.64 and 68.79 correspond to the reflection from (100), (002), (101), (102), (110), (103), (200) and (112) crystal planes of the hexagonal wurtzite zinc oxide structure. The measured d-spacing of 2.81, 2.60, 2.47, 1.91, 1.62, 1.47, 1.40, 1.37, 1.36, 1.30 and 1.23 Å also correspond to the reflection from (100), (002), (101), (102), (110), (103), (200) and (112) crystal planes of the wurtzite structure. All the diffraction peaks agreed with the reported JCPDS card no. 80-0075. Some additional peaks attributable to secondary phase such as zinc iron oxide ($ZnFe_2O_4$) are observed for x = 0.01 to 0.05 at 800 ºC and 1000 ºC according to JCPDS card no 82-1049. It is clearly observed from the XRD patterns that with the increase in temperature of calcinations at 800 to 1000 ºC,
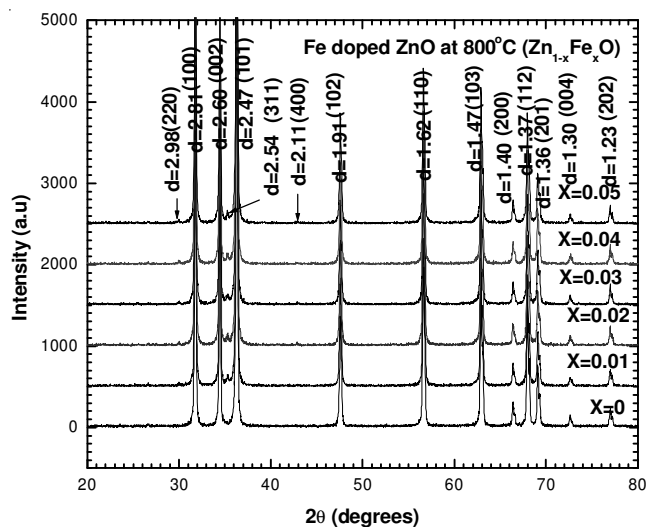
Fig.1(a). XRD patterns of pure ZnO and $Zn_{1-x}Fe_xO$ nanoparticles at 800 ºC, The arrows indicate the formation of secondary ($ZnFe_2O_4$) phase
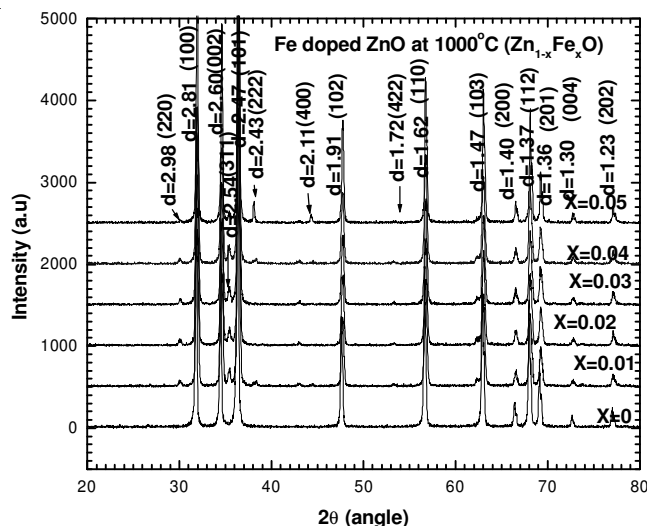
Fig.1(b). XRD patterns of pure ZnO and $Zn_{1-x}Fe_xO$ nanoparticles at 1000 ºC, The arrows indicate the formation of secondary ($ZnFe_2O_4$) phase

the diffraction peaks become sharper and stronger; which suggest that the crystal quality of the nanoparticles are improved and the particles sizes are increased. X-ray diffraction studies confirmed that the synthesized undoped and iron doped zinc oxide nanoparticles were hexagonal wurtzite structure with secondary phase. Thus, it is concluded that the non-uniform distribution of Fe ions into Zn sites. Nevertheless, it is concluded that all of the Fe ions have substituted for Zn in the lattice, as some foreign peaks detected in the patterns.

The mean crystalline size was calculated from the full-width at half-maximum (FWHM) of XRD lines by using the Debye-Scherrer formula:

$$D_{h,k,l} = 0.9\lambda / (\beta_{h,k,l} \cos\theta)$$

where D is the average crystalline diameter, λ is the wavelength in Å, β is the line width at half - maximum and θ is the Bragg angle. We used the most intense peak (101) in the XRD patterns to calculate the average crystalline size. It can be seen that the average size of nanoparticles increases as the heating temperature is increased and decreases as the doping percentage of iron metal is increased. It also indicates that the size of crystallites can be adjusted by controlling the annealing temperature. The calculated values of particles size for undoped and iron doped (1-5 %) ZnO at 800 ºC and 1000 ºC are presented in Table-1. The particles size are in the range of 27 to 39 nm at 800 ºC and 30 to 41 nm at 1000 ºC corresponding to the $Zn_{1-x}Fe_xO$ (x = 0.0 to 0.05) nanoparticles respectively.

TABLE-1 VARIATION OF SIZE WITH TEMPERATURE OF UNDOPED AND Fe DOPED ZnO NANOPARTICLES		
% of doping of Fe	Average size of particles for sample annealed at temperature 800 ºC	Average size of particles for sample annealed at temperature 1000 ºC
0	27	30
1	39	41
2	39	41
3	38	40
4	38	39
5	37	39

Fig. 2. Optical absorption spectra of (a) undoped and (b) iron doped ZnO nanoparticles at 800 ºC.
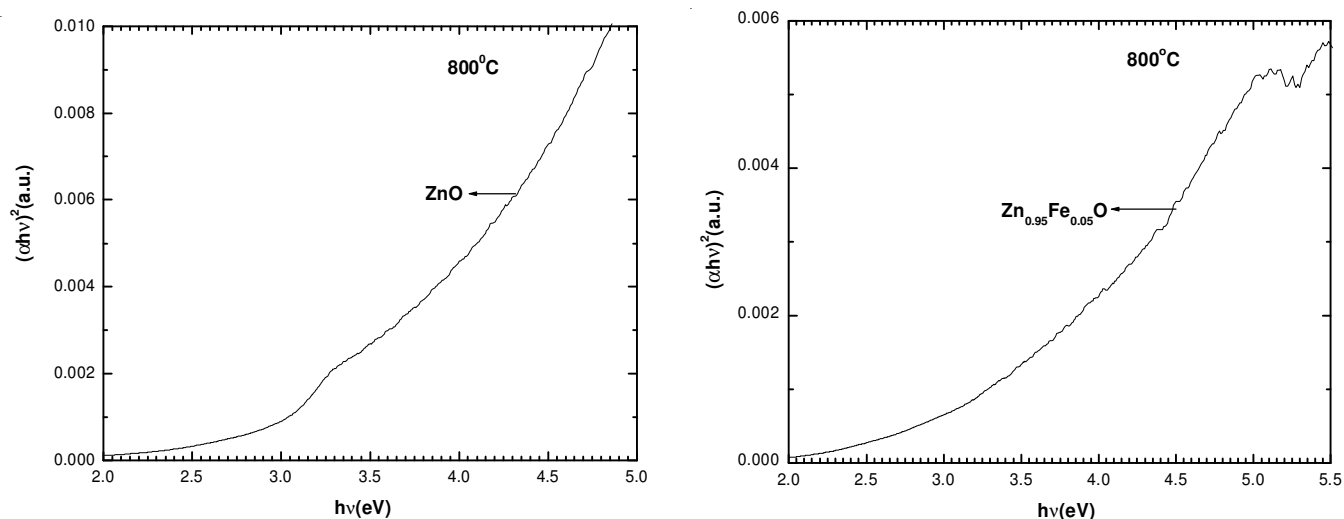
Fig. 3. $(\alpha h\nu)^2$ vs. photon energy (hν) of (a) undoped and (b) iron doped ZnO nanoparticles at 800 ºC.

Optical studies: The optical absorption spectra of $Zn_{1-x}Fe_xO$ (x = 0.00, 0.05) samples by using UV-VIS spectrophotometer in the range of 200 to 800 nm. Absorption edge values of as prepared undoped and iron doped samples at 800 ºC are 427 and 435 nm, respectively as in Fig. 2.

The energy band gap is determined by using the relationship:

$$\alpha = A (h\nu - E_g)^n$$

where hν = Photon energy, α = Absorption coefficient (α = 4πk/λ; k is the absorption index or absorbance, λ is wavelength in nm), E_g = Energy band gap, A = constant , n = 1/2 for allowed direct band gap. Exponent n depends on the type of transition and it may have values 1/2, 2, 3/2 and 3 corresponding to the allowed direct, allowed indirect, forbidden direct and forbidden indirect transitions respectively[24]. The value of band gap at temperature 800 ºC is determined by extrapolating the straight line portion of $(\alpha h\nu)^2 = 0$ axis; as shown in Fig. 3. The band gap decreased from 2.90 to 2.85 eV with iron (5 %) doping at temperature 800 ºC.

Conclusion

Nanocrystals of undoped and iron doped ZnO were successfully synthesized by using a chemical coprecipitation method. XRD analysis showed that the prepared samples were in hexagonal wurtzite structure with secondary phase ($ZnFe_2O_4$). The average size of nanoparticle decreases as the doping percentage of iron metal is increased. The band gap values of prepared undoped and iron doped samples were found to decrease from 2.90 to 2.85 eV. Optical absorption measurements indicated red shift in the absorption band edge upon iron doping.

REFERENCES

1. N. Golego, S.A. Studenikin and M. Cocivera, *J. Electrochem. Soc.,* **147**, 1592 (2000).
2. Y. Lin, Z. Zhang, Z. Tang, F. Yuan and J. Li, *Adv. Mater. Opt. Electron,* **9**, 206 (1999).
3. X. Wang, J. Song, J. Liu and Z.L. Wang, *Science*, **316**, 102 (2007).
4. K. Keren, R.S. Berman, E. Buchstab, U. Sivan and E. Braun, *Science*, **302**, 1380 (2003).
5. K. Nomura, H. Ohta, K. Ueda, T. Kamiya, M. Hirano and H. Hosono, *Science*, **300**, 1269 (2003).
6. T. Nakada, Y. Hirabayashi, T. Tokado, D. Ohmori and T. Mise, *Sol. Energy,* **77**, 739 (2004).
7. S.Y. Lee, E.S. Shim, H.S. Kang, S.S. Pang and J.S. Kang, *Thin Solid Films*, **437**, 31 (2005).
8. R. Könenkamp, R.C. Word and C. Schlegel, *Appl. Phys. Lett.,* **85**, 6004 (2004).
9. S.T. Mckinstry and P. Muralt, *J. Electroceram.,* **12**, 7 (2004).
10. Z.L. Wang, X.Y. Kong, Y. Ding, P. Gao, W. L. Hughes, R. Yang and Y. Zhang, *Adv. Funct. Mater.*, **14**, 943 (2004).
11. M.S. Wagh, L.A. Patil, T. Seth and D.P. Amalnerkar, *Mater. Chem. Phys.*, **84**, 228 (2004).
12. Y. Ushio, M. Miyayama and H. Yanagida, *Sens. Actuators B*, **17**, 221 (1994).
13. H. Harima, *J. Phys. Condens. Matter.*, **16**, S5653 (2004).
14. S. J. Pearton, W. H. Heo, M. Ivill, D. P. Norton and T. Steiner, *Semicond. Sci. Technol.*, **19**, R59 (2004).
15. M.A. Garcia, J.M. Merino, E.F. Pinel, A.J. Quesada, D. Venta, M.L.R. Gonza, G.R. Castro, P. Crespo, J. Llopis, J.M.G. Calbet and A. Hernando, *Nano Lett.*, **7**, 1489 (2007).
16. Q.P. Zhong and E. Matijevic, *J. Mater. Chem.*, **6**, 443 (1996).
17. W. Lingna and M. Mamoun, *J. Mater. Chem.*, **9**, 2871 (1999).
18. D.W. Bhnemann, C. Kormann and M.R. Hoffmann, *J. Phys. Chem.*, **91**, 3789 (1987).
19. Z. Hui, Y. Deren, M. Xiangyang, J. Yujie and X. Jin, *Nanotechnology*, **15**, 622 (2004).
20. J. Zhang, L. D. Sun and J.L. Yin, *Chem. Mater.*, **14** , 4172 (2002).
21. W.J. Li, E.W. Shi and Z.W. Yin, *J. Mater. Sci. Lett.*, **20**, 1381 (2001).
22. S.K. Mandal, *Appl. Phys. Lett.*, **89**,144105 (2006).
23. A.O. Cadar, C. Roman, L. Gagea, B.A. Matei and I. Cernica, *IEEE Xplore.*, 315 (2007).
24. J.I. Pankove, Optical Process in Semiconducters, Prentice-Hall, New Jersey (1971).